This is the accepted manuscript (postprint) of the following article:
N. Zirak, A.B. Jahromi, E. Salahinejad, *Vancomycin release kinetics from Mg–Ca silicate porous microspheres developed for controlled drug delivery*, Ceramics International, 46 (2020) 508-512.
https://doi.org/10.1016/j.ceramint.2019.08.290

Vancomycin release kinetics from Mg-Ca silicate porous microspheres developed for controlled drug delivery

N. Zirak, A. Bolandparvaz Jahromi, E. Salahinejad*

Faculty of Materials Science and Engineering, K. N. Toosi University of Technology, Tehran, Iran

Abstract

In this work, sol-gel derived bredigite ($MgCa_7Si_4O_{16}$), akermanite ($MgCa_2Si_2O_7$), and diopside ($MgCaSi_2O_6$) porous microspheres were loaded with vancomycin, and the release kinetics of this drug from them was evaluated. In this regard, mathematical models of Higuchi, Peppas, Baker-Lonsdale, Hixson-Crowell, first order, and zero order were considered in terms of linear and nonlinear regression analyses. Using the goodness of fitting correlation coefficients, the number of release stages was determined, and then diffusion- and degradation-controlled mechanisms were assigned to each stage. It was found that the diopside microspheres presented a two-step diffusional drug delivery. For akermanite and bredigite, an initial burst diffusion-controlled release followed by a sustained mixed-mode release mechanism of diffusion and degradation was identified, with the domination of the latter especially for bredigite.

Keywords: Sol-gel processes (A); Silicate (D); Biomedical applications (E)

* Corresponding Author: Email Address: <salahinejad@kntu.ac.ir>

This is the accepted manuscript (postprint) of the following article:
N. Zirak, A.B. Jahromi, E. Salahinejad, *Vancomycin release kinetics from Mg–Ca silicate porous microspheres developed for controlled drug delivery*, Ceramics International, 46 (2020) 508-512.
https://doi.org/10.1016/j.ceramint.2019.08.290

1. Introduction

Ceramics are widely used in biomedical applications including bone tissue regeneration medicine and drug delivery systems. In this regard, ceramic microspheres have attracted an increasing level of attention as bone defects fillers, due to their suitable shape and size to fill complex and abnormal defects [1-6]. Porous microspheres used as drug delivery carriers also provide other advantages, such as reducing the usage frequency and side effects of drugs and the ability to control the release of the drugs [7, 8]. Desirable ceramic microspheres used in bone tissue reconstruction and drug delivery systems, while having the ability to control the drug release, should be bioactive and bioresorbable [4].

On the one hand, the ceramic composition is the main parameter that influences its bioactivity, degradability, and biocompatibility. On the other hand, the beneficial effect of some ions released from bioceramics into the tissue environment suggests the incorporation of certain species in tissue-regenerative drug delivery carriers [9-11]. Magnesium as the fourth most abundant cations in the human body is one of these species. The body of a normal adult human contains 1 mole magnesium per 70 kg, where an estimated half of this amount is stored in bone tissues [12]. The encouraging role of magnesium in the adhesion and growth osteoblast cells makes Mg-containing silicates promising for bone tissue repair approaches, in the forms of coating [13-16], scaffold [17, 18], and filler [19-23].

Regarding the drug delivery task, the drug release rate is a key characteristic which is affected by porosity, carrier degradation rate, chemical potential gradient, and the occurrence of physical and chemical processes. In other words, these factors determine the mechanism of drug release from the carriers, which can be recognized by combining precise laboratory data with relevant mathematical models [4, 24-27]. To our knowledge, there are no systematic reports on the study of the mechanism of drug release from Mg-containing silicates, which is

This is the accepted manuscript (postprint) of the following article:
N. Zirak, A.B. Jahromi, E. Salahinejad, *Vancomycin release kinetics from Mg–Ca silicate porous microspheres developed for controlled drug delivery*, Ceramics International, 46 (2020) 508-512.
https://doi.org/10.1016/j.ceramint.2019.08.290

the subject of this paper. In this regard, vancomycin release mechanisms from bredigite ($MgCa_7Si_4O_{16}$), akermanite ($MgCa_2Si_2O_7$), and diopside ($MgCaSi_2O_6$) microspheres were assessed.

2. Materials and methods

Mg-containing silicate powders of bredigite ($MgCa_7Si_4O_{16}$), akermanite ($MgCa_2Si_2O_7$), and diopside ($MgCaSi_2O_6$) were synthesized by sol-gel and calcination processes. Briefly, $Si(OC_2H_5)_4$ was hydrolyzed in H_2O catalyzed by HNO_3 under stirring for 30 min at room temperature. Then, the stoichiometric amounts of $Ca(NO_3)_2{\cdot}4H_2O$ and $MgCl_2{\cdot}6H_2O$ were added and stirred for 5 h, followed by aging at 60 °C for 24 h, drying at 120 °C for 48 h, and calcination at 1300 °C for 3 h.

To fabricate porous microspheres from the synthesized powders, according to Ref. [4], the silicate and carbon (the mean size: 10 μm) powders with a mass ratio of 2:3 were added to a $(C_6H_7NaO_6)_n$ solution. The slurries were dripped into a cross-linking solution of $CaCl_2$, leaving microspheres. The microspheres were then washed with distilled water, dried at 60 °C, and finally sintered at 1000 °C for 2 h to remove carbon and leave porosity. Field-emission scanning electron microscopy (FESEM, TESCAN, MIRA3-XMU, accelerating voltage = 15 kV) was used to characterize the morphology of the microspheres.

The microspheres were centrifuged in a 0.5 $mg.ml^{-1}$ vancomycin-phosphate buffered saline (PBS) solution with the carriers/drug mass ratio of 120:1 for 5 min, followed by drying at room temperature and 60 °C each for 24 h. The drug-loaded microspheres were then incubated into the PBS with a ratio of 60.0 $mg.ml^{-1}$ at 37 °C for 1, 3, 6, 24, 48, 120, and 148 h. The solutions were analyzed by a Thermo Scientific BioMate UV-visible spectrophotometer at the wavelength of 280 nm to determine the concentration of

This is the accepted manuscript (postprint) of the following article:
N. Zirak, A.B. Jahromi, E. Salahinejad, *Vancomycin release kinetics from Mg–Ca silicate porous microspheres developed for controlled drug delivery*, Ceramics International, 46 (2020) 508-512.
https://doi.org/10.1016/j.ceramint.2019.08.290

vancomycin. The experimental data of the drug release were then fitted with mathematical models, including Higuchi [28], Peppas [29], Baker-Lonsdale [30], Hixson-Crowell [31], first order [32], and zero order [32], using Origin Pro 9 and SigmaPlot 14.0 softwares.

3. Results and Discussion

3.1. Experimental

Fig. 1. indicates the macrographs and FESEM micrographs obtained from the prepared microspheres. According to the images, the samples are composed of fairly spherical shaped colonies with the diameter range of 700-1000 μm and the mean diameter of almost 900 μm. According to the high magnification micrographs, the microspheres contain pores of 30-2500 nm in size, with a mean of 35 nm for the nanopores and of 1.5 μm for the micropores. These nanometer-to-micron sized pores provide a platform for the accommodation of vancomycin in the microspheres during the drug loading process.

The cumulative percentage of vancomycin released from the microspheres is shown in Fig. 2. For all the three types of microspheres, a burst release of vancomycin is detected to 6 h, followed by a sustained release to 148 h. Also, at any soaking time, the release level from the different samples is ranked in the following order: bredigite > akermanite > diopside. In other words, the bredigite microspheres present the highest release rates, the diopside microspheres the slowest release rate, and the akermanite microspheres an intermediate release rate between the bredigite and diopside microspheres.

3.2. Modeling

Mathematical modeling of drug release kinetics is a beneficial approach to improve the design of drug delivery systems. These models can be also used to identify the various stages

This is the accepted manuscript (postprint) of the following article:
N. Zirak, A.B. Jahromi, E. Salahinejad, *Vancomycin release kinetics from Mg–Ca silicate porous microspheres developed for controlled drug delivery*, Ceramics International, 46 (2020) 508-512.
https://doi.org/10.1016/j.ceramint.2019.08.290

and mechanism of drug release from carriers. Various types of carriers like microspheres, mesoporous materials, and nanoparticles exhibit different stages of drug release [33-35]. For example, vancomycin-containing sol-gel processed silica microspheres show three stages of the drug release: a first delay phase, a second release phase, followed by a third stage with a slower release [6]. The models have been established in accordance to the different mechanisms of drug release, including diffusion, dissolution, or both [36]. The fitting quality of the experimental release data with some relevant models is evaluated to determine the drug release mechanisms, in terms of the correlation coefficient of regression (R_c) [37, 38].

First, the Higuchi model [28] was used to evaluate the release of vancomycin from the bredigite, akermanite, and diopside microspheres, as follows:

$$M_t = \sqrt{\frac{D\varepsilon}{\tau}(2A - \varepsilon C_s)C_s t} \quad (1)$$

where M_t is the amount of drug released at time t by surface unity, A is the initial concentration of the drug, ε is the matrix porosity, τ is the tortuosity factor of the capillary system, C_s is the drug solubility in the matrix/excipient medium, and D is the diffusion constant of the drug molecules in that liquid. This equation can be expressed as below:

$$Q = \frac{M_t}{M_\infty} = k\sqrt{t} \quad (2)$$

where Q is the fraction of drug release, M_∞ is the cumulative drug release at infinite time, and k is a constant. Given that the correlation coefficients obtained from the single-stage regression of the Higuchi model, i.e. over the entire range of the drug release, were far from unit for all of the three microspheres, it was understood that the release of the drug from the microspheres involves several steps. Considering a two-stage regression with a cut-off time selected on the criterion of the proximity of the fitting correlation coefficients to unit, the experimental data of release was divided into two groups (0-6 h and 6-148 h) and

This is the accepted manuscript (postprint) of the following article:
N. Zirak, A.B. Jahromi, E. Salahinejad, *Vancomycin release kinetics from Mg–Ca silicate porous microspheres developed for controlled drug delivery*, Ceramics International, 46 (2020) 508-512.
https://doi.org/10.1016/j.ceramint.2019.08.290

independently regressed with the Higuchi models, as shown in Fig. 3a. The values of the correlation coefficient for this two-stage regression indicate the excellency of the fitting process (Table 1). In accordance to the literature, the application of the Higuchi model points out different stages of vancomycin release from various carriers, for instance, a mono-step process from microporous polymer-impregnated brushite [39], two-step processes from silica microspheres [6] and bioactive glass nanoparticles [40], and a three-step process from silica granules [6]. That is, the number of vancomycin release stages is the carrier-dependent, not drug-dependent.

To determine the mechanism of the drug release from the different microspheres at each stage, the Peppas model [41] was used:

$$Q = kt^n \quad (3)$$

where *n* is an indicator of the mechanism of drug release, as classified into three modes: diffusion, degradation and a mixed of them. According to this model, for spherical carriers, n = 0.43 indicates a diffusion-controlled release, n = 1 depicts a drug release based on degradation, and when the value is between 0.43 and 1, the carriers show an anomalous transport behavior including degradation and diffusion [36]. It is noteworthy that the Peppas model has been developed to describe drug release from polymeric carriers; however, it is also used for ceramic porous systems when the mechanism of drug release is unknown [39]. The fitting plot of the drug release data from the microspheres with the Peppas model is demonstrated in Fig. 3b, and the related parameters are listed in Table 2. For the first stage of release, the correlation coefficients more than 0.98 which means excellent fitting were obtained at n = 0.43 for all the carriers, suggesting the domination of Fickian diffusion. For the second stage that happens at a slower rate, using the Peppas equation, n = 0.43 for the diopside microspheres and n = 0.45 for the akermanite and bredigite microspheres yield the

This is the accepted manuscript (postprint) of the following article:
N. Zirak, A.B. Jahromi, E. Salahinejad, *Vancomycin release kinetics from Mg–Ca silicate porous microspheres developed for controlled drug delivery*, Ceramics International, 46 (2020) 508-512.
https://doi.org/10.1016/j.ceramint.2019.08.290

best fitting results. That is, the second stage of vancomycin release is controlled by diffusion for diopside and by a mixed mode of diffusion and degradation for akermanite and bredigite.

To verify the conclusions drawn from the Peppas analysis on the drug transport mechanisms, the following models were also correlated with the experimental data and the fitting merit was evaluated:

i) Baker and Lonsdale equation [30] for a spherical matrix which is a development of the Higuchi model and describes diffusion-controlled drug release cases:

$$\frac{3}{2}\left[1-\left(1-\frac{M_t}{M_\infty}\right)^{\frac{2}{3}}\right]-\frac{M_t}{M_\infty}=kt \quad (4)$$

ii) Hixson and Crowell cube-root equation [31] which is used for systems that show dissolution-controlled behaviors:

$$\sqrt[3]{1-\frac{M_t}{M_\infty}}=-kt \quad (5)$$

iii) First order release [32] in which the activity of the drug in the matrix is reduced exponentially, with the consideration of the geometry and dissolution of the carrier:

$$\ln\left(1-\frac{M_t}{M_\infty}\right)=-kt \quad (6)$$

iv) Zero order release [32] which is used for systems with degradation-controlled drug release mechanisms:

$$\frac{M_t}{M_\infty}=kt \quad (7)$$

The fitting parameters of the experimental data with these four equations are listed in Table 3. Comparing the correlation coefficients of these models in the first stage of release, it is found that the best fitting is related to the diffusion-controlled Baker-Lonsdale equation for all the carriers. This is in good agreement with the mechanism identified by the Peppas fitting. The diffusion-controlled mechanism of the drug release at this stage (i.e. the

This is the accepted manuscript (postprint) of the following article:
N. Zirak, A.B. Jahromi, E. Salahinejad, *Vancomycin release kinetics from Mg–Ca silicate porous microspheres developed for controlled drug delivery*, Ceramics International, 46 (2020) 508-512.
https://doi.org/10.1016/j.ceramint.2019.08.290

negligible contribution of dissolution) is well supported by the fact that after one day of soaking in a simulated body fluid, the weight loss of bredigite, akermanite, and diopside disks is lower than 0.85, 0.5, and 0.5 %, respectively [42]. Since the first stage of the drug release from all the carriers lasts for 6 h, the degradation amount of the microspheres during this stage is insignificant and has no considerable effect on the drug release. The fitting analysis on the second stage of release demonstrates that the highest correlation coefficient for diopside is related to the diffusion-based Baker-Lonsdale model, which confirms the diffusional mechanism realized from the Peppas analysis. Regarding the bredigite and akermanite carriers, on the one hand, the Peppas analysis pointed out a combined release mechanism of degradation and diffusion at this stage. On the other hand, the Baker-Lonsdale-to-Hixson-Crowell correlation coefficient ratio for bredigite is lower than that for akermanite. Considering that the Baker-Lonsdale and Hixson-Crowell models are diffusional- and dissolution-based, respectively, it is realized that the contribution of the degradation mechanism for bredigite is more than that for akermanite.

It is eventually concluded that the contribution of degradation to the drug release comparatively ranks as: bredigite > akermanite > diopside, as a result of the difference of the degradation rate in the same ranking. This is compatible with the report of Wu and Cheng [42] comparing the *in vitro* weight loss of bredigite, akermanite, and diopside immersed in a simulated body fluid. This ranking is attributed to the relative amounts of SiO_2/CaO and MgO/CaO in the different ceramics, where bredigite ($MgCa_7Si_4O_{16}$ or $4SiO_2$-7CaO-MgO) has the lowest, diopside ($MgCaSi_2O_6$ or $2SiO_2$-CaO-MgO) possesses the highest, and akermanite ($MgCa_2Si_2O_7$ or $2SiO_2$-2CaO-MgO) enjoys the intermediate values of these essential constitutes. The higher content of SiO_2 ensures the connectivity and thereby stability of the silicate network. Also, the higher bond energy of Mg-O than Ca-O limits the release of

This is the accepted manuscript (postprint) of the following article:
N. Zirak, A.B. Jahromi, E. Salahinejad, *Vancomycin release kinetics from Mg–Ca silicate porous microspheres developed for controlled drug delivery*, Ceramics International, 46 (2020) 508-512.
https://doi.org/10.1016/j.ceramint.2019.08.290

both Mg and Ca ions [42, 43]. This is in good agreement with that fact that the degradability of silicate ceramics is in inverse proportional to the activation energy of silicon release, where the activation energy is increased with amounts of both SiO_2 and MgO in the SiO_2-CaO-MgO system [42, 44].

4. Conclusions

In this work, vancomycin release from bredigite, akermanite, and diopside porous microspheres was studied. Considering the results of this work in addition to the literature, it was concluded that the number of vancomycin release stages is determined by specifications of the carriers, not drug. Additionally, according to experimental and modeling analyses, the drug transfer from the silicate carriers consisted of two steps: an initial burst release followed by a slow sustained release. The first stage of release for all the carriers was based on a diffusion-controlled mechanism. At the second stage of release, the drug-loaded diopside microspheres again exhibited a diffusion-controlled release of vancomycin. However, a mixed mode of diffusion and degradation was identified to control the second stage of release from the bredigite and akermanite microspheres, where degradation was dominant for both.

Acknowledgments

The Iran National Science Foundation is acknowledged for the support of this work under the grant number of 97006529.

References

[1] W. Paul, C.P. Sharma, Ceramic drug delivery: a perspective, Journal of biomaterials applications, 17 (2003) 253-264.

[2] S. Hulbert, F. Young, R. Mathews, J. Klawitter, C. Talbert, F. Stelling, Potential of ceramic materials as permanently implantable skeletal prostheses, Journal of biomedical materials research, 4 (1970) 433-456.
[3] T.J. Webster, C. Ergun, R.H. Doremus, R.W. Siegel, R. Bizios, Enhanced functions of osteoblasts on nanophase ceramics, Biomaterials, 21 (2000) 1803-1810.
[4] C. Wu, H. Zreiqat, Porous bioactive diopside (CaMgSi2O6) ceramic microspheres for drug delivery, Acta biomaterialia, 6 (2010) 820-829.
[5] B. Flautre, C. Maynou, J. Lemaitre, P. Van Landuyt, P. Hardouin, Bone colonization of β–TCP granules incorporated in brushite cements, Journal of Biomedical Materials Research: An Official Journal of The Society for Biomaterials, The Japanese Society for Biomaterials, and The Australian Society for Biomaterials and the Korean Society for Biomaterials, 63 (2002) 413-417.
[6] S. Radin, T. Chen, P. Ducheyne, The controlled release of drugs from emulsified, sol gel processed silica microspheres, Biomaterials, 30 (2009) 850-858.
[7] K. Sahil, M. Akanksha, S. Premjeet, A. Bilandi, B. Kapoor, Microsphere: A review, Int. J. Res. Pharm. Chem, 1 (2011) 1184-1198.
[8] M. Sharma, S.K. Dev, M. Kumar, A.K. Shukla, Microspheres as suitable drug carrier in Sustained Release Drug Delivery: An overview, Asian Journal of Pharmacy and Pharmacology, 4 (2018) 102-108.
[9] A. Hoppe, N.S. Güldal, A.R. Boccaccini, A review of the biological response to ionic dissolution products from bioactive glasses and glass-ceramics, Biomaterials, 32 (2011) 2757-2774.
[10] A. Lansdown, Zinc in the healing wound, The Lancet, 347 (1996) 706-707.
[11] A. Rezania, K.E. Healy, Integrin subunits responsible for adhesion of human osteoblast-like cells to biomimetic peptide surfaces, Journal of orthopaedic research, 17 (1999) 615-623.
[12] S.E. Ruiz-Hernandez, R. Grau-Crespo, N. Almora-Barrios, M. Wolthers, A.R. Ruiz-Salvador, N. Fernandez, N.H. de Leeuw, Mg/Ca partitioning between aqueous solution and aragonite mineral: a molecular dynamics study, Chemistry–A European Journal, 18 (2012) 9828-9833.
[13] R. Vahedifard, E. Salahinejad, Microscopic and spectroscopic evidences for multiple ion-exchange reactions controlling biomineralization of CaO. MgO. 2SiO2 nanoceramics, Ceramics International, 43 (2017) 8502-8508.
[14] E. Salahinejad, R. Vahedifard, Deposition of nanodiopside coatings on metallic biomaterials to stimulate apatite-forming ability, Materials & Design, 123 (2017) 120-127.
[15] S. Rastegari, E. Salahinejad, Surface modification of Ti-6Al-4V alloy for osseointegration by alkaline treatment and chitosan-matrix glass-reinforced nanocomposite coating, Carbohydrate polymers, 205 (2019) 302-311.
[16] S. Karimi, E. Salahinejad, E. Sharifi, A. Nourian, L. Tayebi, Bioperformance of chitosan/fluoride-doped diopside nanocomposite coatings deposited on medical stainless steel, Carbohydrate polymers, 202 (2018) 600-610.
[17] M. Shahrouzifar, E. Salahinejad, Strontium doping into diopside tissue engineering scaffolds, Ceramics International, 45 (2019) 10176-10181.
[18] M. Shahrouzifar, E. Salahinejad, E. Sharifi, Co-incorporation of strontium and fluorine into diopside scaffolds: Bioactivity, biodegradation and cytocompatibility evaluations, Materials Science and Engineering: C, 103 (2019) 109752.
[19] M. Diba, F. Tapia, A.R. Boccaccini, L.A. Strobel, Magnesium-containing bioactive glasses for biomedical applications, International Journal of Applied Glass Science, 3 (2012) 221-253.
[20] M.J. Baghjeghaz, E. Salahinejad, Enhanced sinterability and in vitro bioactivity of diopside through fluoride doping, Ceramics International, 43 (2017) 4680-4686.
[21] N. Esmati, T. Khodaei, E. Salahinejad, E. Sharifi, Fluoride doping into SiO2-MgO-CaO bioactive glass nanoparticles: bioactivity, biodegradation and biocompatibility assessments, Ceramics International, 44 (2018) 17506-17513.

[22] H. Rahmani, E. Salahinejad, Incorporation of monovalent cations into diopside to improve biomineralization and cytocompatibility, Ceramics International, 44 (2018) 19200-19206.
[23] E. Salahinejad, M.J. Baghjeghaz, Structure, biomineralization and biodegradation of Ca-Mg oxyfluorosilicates synthesized by inorganic salt coprecipitation, Ceramics International, 43 (2017) 10299-10306.
[24] A. Ebadi, A. Rafati, Development of Novel Biodegradable Enrofloxacin–Silica Composite for In Vitro Drug Release Kinetic Studies, Journal of Polymers and the Environment, 26 (2018) 3404-3411.
[25] N.A. Peppas, B. Narasimhan, Mathematical models in drug delivery: How modeling has shaped the way we design new drug delivery systems, Journal of Controlled Release, 190 (2014) 75-81.
[26] V. Papadopoulou, K. Kosmidis, M. Vlachou, P. Macheras, On the use of the Weibull function for the discernment of drug release mechanisms, International journal of pharmaceutics, 309 (2006) 44-50.
[27] S. Fredenberg, M. Wahlgren, M. Reslow, A. Axelsson, The mechanisms of drug release in poly (lactic-co-glycolic acid)-based drug delivery systems—a review, International journal of pharmaceutics, 415 (2011) 34-52.
[28] T. Higuchi, Mechanism of sustained-action medication. Theoretical analysis of rate of release of solid drugs dispersed in solid matrices, Journal of pharmaceutical sciences, 52 (1963) 1145-1149.
[29] P.L. Ritger, N.A.J.J.o.c.r. Peppas, A simple equation for description of solute release I. Fickian and non-fickian release from non-swellable devices in the form of slabs, spheres, cylinders or discs, 5 (1987) 23-36.
[30] R. Baker, H. Lonsdale, In AC Tanquary and RE Lacey (eds.), Controlled Release of Biologically Active Agents, Plenum Press, New York and London, 1974.
[31] A. Hixson, J. Crowell, Dependence of reaction velocity upon surface and agitation, Industrial & Engineering Chemistry, 23 (1931) 923-931.
[32] A.L.W. Po, L. Wong, C. Gilligan, Characterisation of commercially available theophylline sustained- or controlled-release systems: in-vitro drug release profiles, International Journal of Pharmaceutics, 66 (1990) 111-130.
[33] J.M. Unagolla, A.C.J.E.J.o.P.S. Jayasuriya, Drug transport mechanisms and in vitro release kinetics of vancomycin encapsulated chitosan-alginate polyelectrolyte microparticles as a controlled drug delivery system, 114 (2018) 199-209.
[34] B.G. Trewyn, S. Giri, I.I. Slowing, V.S.-Y.J.C.c. Lin, Mesoporous silica nanoparticle based controlled release, drug delivery, and biosensor systems, (2007) 3236-3245.
[35] A.M. El-Kady, M.M. Farag, A.M.J.E.J.o.P.S. El-Rashedi, Bioactive glass nanoparticles designed for multiple deliveries of lithium ions and drugs: Curative and restorative bone treatment, 91 (2016) 243-250.
[36] H. Qu, S. Bhattacharyya, P. Ducheyne, Sol–Gel Processed Oxide Controlled Release Materials, Comprehensive Biomaterials, 4 (2017) 617-643.
[37] D. Lu, K. Abu-Izza, F. Mao, Nonlinear data fitting for controlled release devices: an integrated computer program, International journal of pharmaceutics, 129 (1996) 243-251.
[38] P. Costa, J.M.S. Lobo, Modeling and comparison of dissolution profiles, European journal of pharmaceutical sciences, 13 (2001) 123-133.
[39] U. Gbureck, E. Vorndran, J.E. Barralet, Modeling vancomycin release kinetics from microporous calcium phosphate ceramics comparing static and dynamic immersion conditions, Acta biomaterialia, 4 (2008) 1480-1486.
[40] A.M. El-Kady, M.M. Farag, A.M. El-Rashedi, Bioactive glass nanoparticles designed for multiple deliveries of lithium ions and drugs: Curative and restorative bone treatment, European Journal of Pharmaceutical Sciences, 91 (2016) 243-250.

This is the accepted manuscript (postprint) of the following article:
N. Zirak, A.B. Jahromi, E. Salahinejad, *Vancomycin release kinetics from Mg–Ca silicate porous microspheres developed for controlled drug delivery*, Ceramics International, 46 (2020) 508-512.
https://doi.org/10.1016/j.ceramint.2019.08.290

[41] P.L. Ritger, N.A. Peppas, A simple equation for description of solute release I. Fickian and non-fickian release from non-swellable devices in the form of slabs, spheres, cylinders or discs, Journal of controlled release, 5 (1987) 23-36.
[42] C. Wu, J. Chang, Degradation, bioactivity, and cytocompatibility of diopside, akermanite, and bredigite ceramics, Journal of Biomedical Materials Research Part B: Applied Biomaterials, 83 (2007) 153-160.
[43] M. Vallet-Regi, A. Salinas, J. Roman, M. Gil, Effect of magnesium content on the in vitro bioactivity of CaO-MgO-SiO 2-P 2 O 5 sol-gel glasses, Journal of Materials Chemistry, 9 (1999) 515-518.
[44] D. Arcos, D. Greenspan, M. Vallet-Regí, A new quantitative method to evaluate the in vitro bioactivity of melt and sol-gel-derived silicate glasses, Journal of Biomedical Materials Research Part A, 65 (2003) 344-351.

This is the accepted manuscript (postprint) of the following article:
N. Zirak, A.B. Jahromi, E. Salahinejad, *Vancomycin release kinetics from Mg–Ca silicate porous microspheres developed for controlled drug delivery*, Ceramics International, 46 (2020) 508-512.
https://doi.org/10.1016/j.ceramint.2019.08.290

Figures

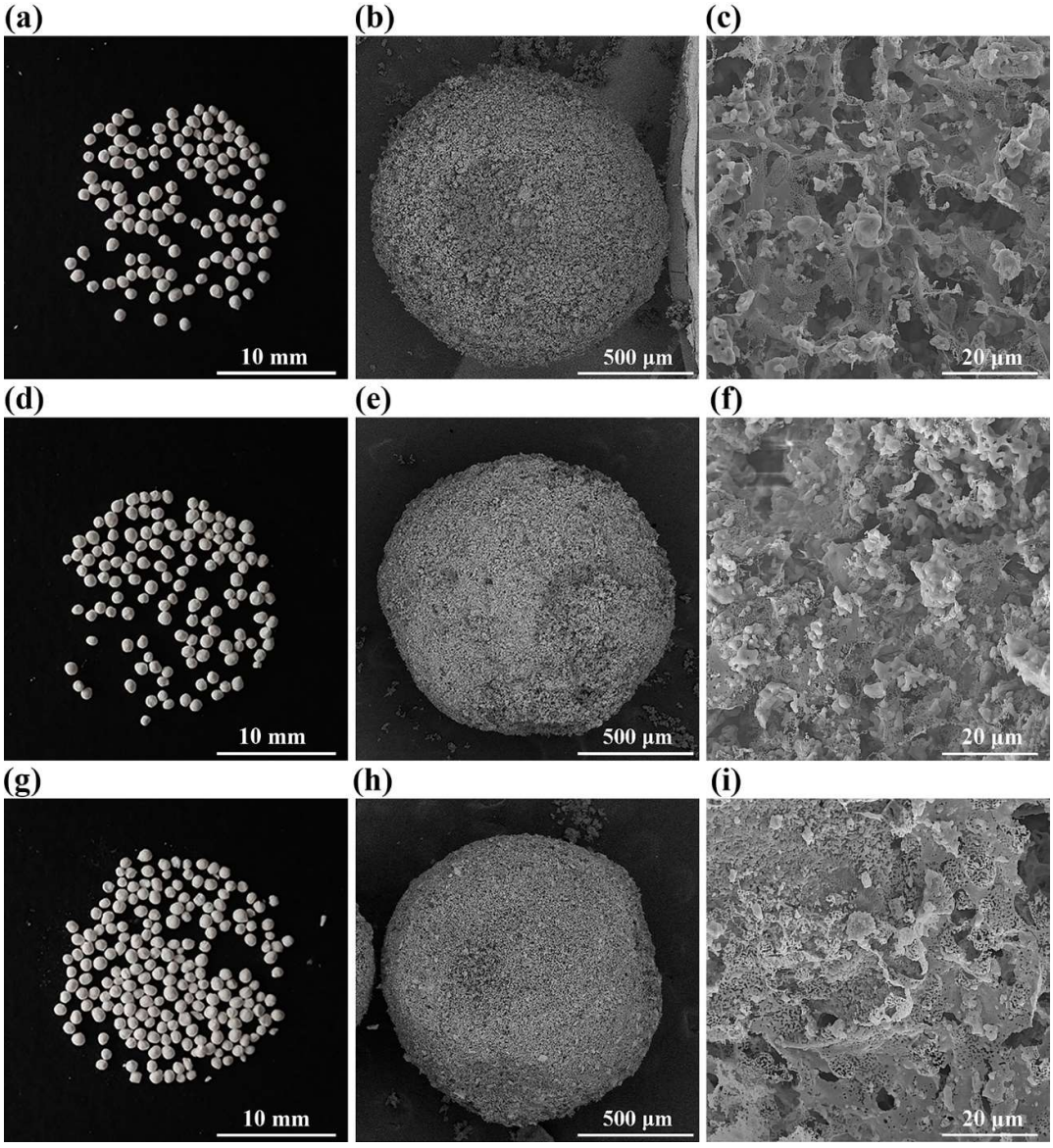

Fig. 1. Macrographs and FESEM micrographs of the microspheres in two magnifications: bredigite (a, b and c), akermanite (d, e and f), and diopside (g, h and i).

This is the accepted manuscript (postprint) of the following article:
N. Zirak, A.B. Jahromi, E. Salahinejad, *Vancomycin release kinetics from Mg–Ca silicate porous microspheres developed for controlled drug delivery*, Ceramics International, 46 (2020) 508-512.
https://doi.org/10.1016/j.ceramint.2019.08.290

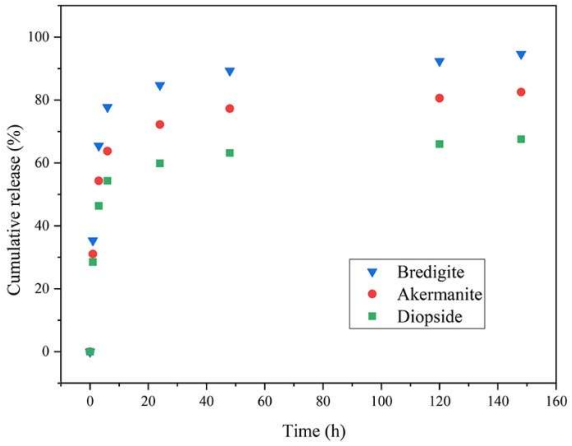

Fig. 2. Measured release percentage of vancomycin from the microspheres.

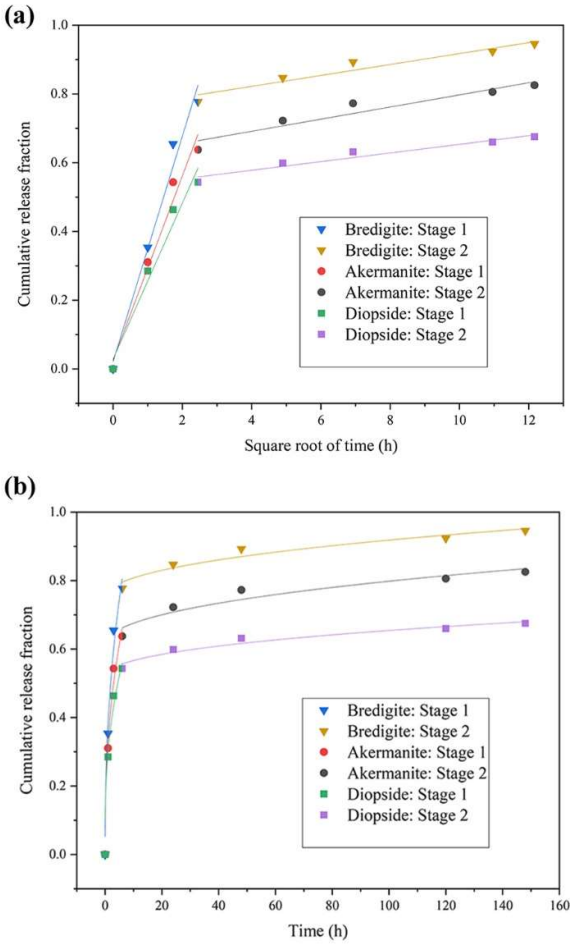

Fig. 3. Fitted Higuchi (a) and Peppas (b) plots of vancomycin release from the microspheres.

This is the accepted manuscript (postprint) of the following article:
N. Zirak, A.B. Jahromi, E. Salahinejad, *Vancomycin release kinetics from Mg–Ca silicate porous microspheres developed for controlled drug delivery*, Ceramics International, 46 (2020) 508-512.
https://doi.org/10.1016/j.ceramint.2019.08.290

Tables

Table 1. Parameters obtained from the Higuchi fitting for the first and second stages of the drug release from the bredigite, akermanite, and diopside microspheres.

Bredigite				**Akermanite**				**Diopside**			
Stage 1		**Stage 2**		**Stage 1**		**Stage 2**		**Stage 1**		**Stage 2**	
k	R_c	k	R_c	k	R_c	k	R_c	k	R_c	k	R_c
0.3300	0.99	0.0159	0.96	0.2700	0.99	0.0152	*0.95*	0.2300	0.98	0.0126	0.97

Table 2. Parameters derived from the Peppas fitting for the first and second stages of the drug release from the bredigite, akermanite, and diopside microspheres.

	Stage 1			**Stage 2**			
Sample	k	**n**	R_c	**Intercept**	K	**n**	R_c
Bredigite	0.37	0.43	0.98	**0.75**	0.0216	0.45	0.97
Akermanite	0.28	0.43	0.98	**0.62**	0.0215	0.45	0.96
Diopside	0.22	0.43	0.98	**0.51**	0.0193	0.43	0.98

This is the accepted manuscript (postprint) of the following article:
N. Zirak, A.B. Jahromi, E. Salahinejad, *Vancomycin release kinetics from Mg–Ca silicate porous microspheres developed for controlled drug delivery*, Ceramics International, 46 (2020) 508-512.
https://doi.org/10.1016/j.ceramint.2019.08.290

Table 3. Regression correlation coefficient values derived from the different fitting for the first and second stages of the drug release from the bredigite, akermanite, and diopside microspheres.

Model	R_c for bredigite		R_c for akermanite		R_c for diopside	
	Stage 1	Stage 2	Stage 1	Stage 2	Stage 1	Stage 2
Baker-Lonsdale	0.99	0.96	0.99	0.95	0.99	0.96
Hixson-Crowell	0.96	0.86	0.92	0.83	0.88	0.87
First order	0.98	0.64	0.95	0.79	0.91	0.80
Zero order	0.98	0.63	0.83	0.80	0.80	0.78